

Editorial Manager(tm) for International Journal of Earth Sciences
Manuscript Draft

Manuscript Number:

Title: Magnetic fabric of Pleistocene continental clays from the hanging-wall of an active low-angle normal fault (Altotiberina Fault, Italy)

Article Type: Original Paper

Keywords: Anisotropy of magnetic susceptibility; magnetic fabric; detachment fault; low-angle normal fault; Altotiberina fault; central Apennines

Corresponding Author: Marco Maffione, Ph.D.

Corresponding Author's Institution: University of Plymouth

First Author: Marco Maffione, Ph.D.

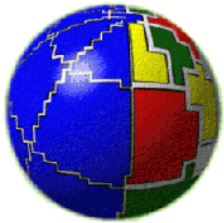
Order of Authors: Marco Maffione, Ph.D.;Stefano Pucci, Ph.D.;Leonardo Sagnotti, Ph.D.;Fabio Speranza, Ph.D.

Abstract: Anisotropy of magnetic susceptibility (AMS) represents a valuable proxy able to detect subtle strain effects in very weakly deformed sediments. During the last decades a large number of AMS studies have documented that in compressive tectonic settings the maximum susceptibility axes (i.e. the magnetic lineations) are parallel to fold axes (and thrust faults) and local bedding strikes, while in extensional regimes they are perpendicular to the normal faults and, thus, parallel to the strata dip directions.

One of the most striking active tectonic structures of the northern Apennines is represented by the Altotiberina Fault (ATF), a NE-dipping low-angle normal fault bounding the High Tiber Valley. The ATF represents a primary detachment of the Plio-Quaternary extensional tectonics affecting the Apennine belt. The long-lasting activity of the ATF produced 5 km of total displacement and up to 1200-m-thick basin infill of syn-tectonic, sandy-clayey continental succession. Thus, the AMS analysis of the sediments lying above the ATF represents a unique opportunity to document the strain field affecting the hanging-wall of low-angle normal faults.

We collected 129 oriented cores at 12 different localities within the High Tiber Valley, and measured the AMS with a spinner Multi-Function Kappabridge. Most of the sites show a magnetic fabric typical of sediments at the earliest stages of deformation, characterized by oblate AMS ellipsoids and a well defined magnetic lineation, while prolate AMS ellipsoids at two sites are suggestive of pervasive tectonic effects. The magnetic lineation is well-developed at all sites and has a prevailing N-S direction. At five sites the bedding is tilted and the magnetic lineation is sub-parallel to local bed-strikes, implying that these sites underwent a maximum horizontal shortening along an E-W direction. At two sites the magnetic lineation is sub-perpendicular to the trend of the ATF, and may be related to extensional strain.

Our results reveal the existence of both compressional and extensional structures at the hangingwall of the ATF, and suggest that the early Pleistocene sequence of the High Tiber Valley is arranged in gently, local folds (hardly visible in the field) ~N-S trending. We interpret these compressive structures as the result of local superficial stress induced by irregularities of the fault plane at depth. Accordingly, the strain field we documented from the High Tiber Valley can not be used to infer the regional tectonic regime acting during the ATF activity. We conclude that the long-lasting debate on the extensional vs. compressional Plio-Quaternary tectonics of the Apennines orogenic belt should be revised evaluating the importance of compressional structures resulting by local effects.



Istituto Nazionale di Geofisica e Vulcanologia

Via di Vigna Murata 605 - 00143 Roma

Dr. Marco Maffione

e-mail: marco.maffione@plymouth.ac.uk

September 29th, 2010

Prof. Manish Mamtani
Guest Editor of the
International Journal of Earth Sciences

Dear Prof. Mamtani,

Thank you for the invitation letter you sent to Prof. Leonardo Sagnotti. It has been a pleasure and an honour for us to have the opportunity to contribute to the thematic issue of the *International Journal of Earth Sciences* entitled "Rocks, fabrics and magnetic anisotropy" in honour of Prof. Hrouda.

We are pleased to send you the electronic version of the paper « Magnetic fabric of Pleistocene continental clays from the hanging-wall of an active low-angle normal fault (Altotiberina Fault, Italy)», by Marco Maffione, Stefano Pucci, Leonardo Sagnotti and Fabio Speranza, that I would like to submit to the thematic issue of the *International Journal of Earth Sciences* entitled "Rocks, fabrics and magnetic anisotropy".

No part of this paper has been published or submitted elsewhere.

Yours sincerely,

Marco Maffione (on behalf of the co-authors)

Magnetic fabric of Pleistocene continental clays from the hanging-wall of an active low-angle normal fault (Altotiberina Fault, Italy)

Marco Maffione ^{1,2}, Stefano Pucci ¹, Leonardo Sagnotti ¹, Fabio Speranza ¹

¹ Istituto Nazionale di Geofisica e Vulcanologia, Rome, Italy.

² Now at the School of Geography, Earth and Environmental Sciences (SoGEES), University of Plymouth, Plymouth, UK

1 **Abstract**

2 Anisotropy of magnetic susceptibility (AMS) represents a valuable proxy able to detect subtle strain
3 effects in very weakly deformed sediments. During the last decades a large number of AMS studies
4 have documented that in compressive tectonic settings the maximum susceptibility axes (i.e. the
5 magnetic lineations) are parallel to fold axes (and thrust faults) and local bedding strikes, while in
6 extensional regimes they are perpendicular to the normal faults and, thus, parallel to the strata dip
7 directions.

8 One of the most striking active tectonic structures of the northern Apennines is represented by the
9 Altotiberina Fault (ATF), a NE-dipping low-angle normal fault bounding the High Tiber Valley.
10 The ATF represents a primary detachment of the Plio-Quaternary extensional tectonics affecting the
11 Apennine belt. The long-lasting activity of the ATF produced 5 km of total displacement and up to
12 1200-m-thick basin infill of syn-tectonic, sandy-clayey continental succession. Thus, the AMS
13 analysis of the sediments lying above the ATF represents a unique opportunity to document the
14 strain field affecting the hanging-wall of low-angle normal faults.

15 We collected 129 oriented cores at 12 different localities within the High Tiber Valley, and
16 measured the AMS with a spinner Multi-Function Kappabridge. Most of the sites show a magnetic
17 fabric typical of sediments at the earliest stages of deformation, characterized by oblate AMS
18 ellipsoids and a well defined magnetic lineation, while prolate AMS ellipsoids at two sites are
19 suggestive of pervasive tectonic effects. The magnetic lineation is well-developed at all sites and
20 has a prevailing N-S direction. At five sites the bedding is tilted and the magnetic lineation is sub-
21 parallel to local bed-strikes, implying that these sites underwent a maximum horizontal shortening
22 along an E-W direction. At two sites the magnetic lineation is sub-perpendicular to the trend of the
23 ATF, and may be related to extensional strain.

24 Our results reveal the existence of both compressional and extensional structures at the hangingwall
25 of the ATF, and suggest that the early Pleistocene sequence of the High Tiber Valley is arranged in
26 gently, local folds (hardly visible in the field) ~N-S trending. We interpret these compressive

27 structures as the result of local superficial stress induced by irregularities of the fault plane at depth.
28 Accordingly, the strain field we documented from the High Tiber Valley can not be used to infer the
29 regional tectonic regime acting during the ATF activity. We conclude that the long-lasting debate
30 on the extensional vs. compressional Plio-Quaternary tectonics of the Apennines orogenic belt
31 should be revised evaluating the importance of compressional structures resulting by local effects.

32

33 1. **Introduction**

34 The analysis of anisotropy of magnetic susceptibility (AMS) is a non-destructive, relatively
35 fast, and accurate method for studying petrofabrics. It has long been established that AMS data may
36 represent a valuable strain proxy and can be used to detect subtle strain effects in sediments at the
37 first stages of deformation (see reviews by Hrouda, 1982; Borradaile, 1988; Tarling and Hrouda,
38 1993; Borradaile and Henry, 1997; Borradaile and Jackson, 2004). As a matter of fact, AMS is
39 extremely sensitive to incipient strain in fine-grained sediments and it develops well before other
40 macro- and mesoscopic strain features (such as cleavage) can be observed in the field.

41 Therefore, the analysis of the AMS in weakly deformed sediments has been increasingly used
42 during the past few decades to better constrain the structural setting of mountain belts. It has been
43 shown that if there is a stress field acting on a sediment, causing progressive strain, the primary
44 AMS fabric is modified according to the nature and the extent of the deformation (e.g. Graham,
45 1966; Sagnotti and Speranza, 1993; Sagnotti et al., 1998; Parés et al, 1999; Parés, 2004). Although
46 no simple relation exists between degree of anisotropy and strain magnitude, it has been
47 demonstrated that the directions of the principal axes of the magnetic susceptibility ellipsoid are
48 parallel to directions of the principal axes of the rock strain ellipsoid, and that the AMS may be
49 used to delineate the preferred orientation of phyllosilicate grains in mudstones produced by
50 compaction and tectonic processes (Hrouda, 1982; Tarling and Hrouda, 1993). Such
51 correspondence makes AMS a fundamental tool to unravel the tectonic setting of weakly deformed
52 mudstones lacking visible strain markers.

53 In Italy, there has been an extensive investigation of mildly deformed marine clays of
54 Oligocene to Pleistocene age deposited both in the Alpine-Apennine-Maghrebide belt (Sagnotti and
55 Speranza, 1993; Mattei et al., 1997, 1999; Sagnotti et al., 1998; Maffione et al., 2008), and in the
56 intraplate setting of Sardinia (Faccenna et al., 2002). These studies have clearly demonstrated that
57 the magnetic lineation (i.e., the maximum susceptibility axis) trends parallel to fold axes in foredeep
58 basins of the Apennine-Maghrebide chain, and it is thus roughly orthogonal to the direction of
59 maximum horizontal shortening (Sagnotti et al., 1998; Speranza et al., 1999). Conversely, the post-
60 collisional syn-rift basins developed at the rear of the Apennine chain yielded a magnetic lineation
61 sub-parallel to the direction of local extension (Sagnotti et al., 1994; Mattei et al., 1999; Cifelli et
62 al., 2004).

63 However, AMS studies in extensional settings of Italy were systematically performed so far
64 in basins bounded and cut by high-angle ($\sim 60^\circ$) extensional faults, while recently it has been found
65 that one of the most significant active tectonic structures of the northern Apennines is a NE-dipping
66 low-angle ($\sim 20^\circ$) normal fault known as Altotiberina Fault (ATF, Brozzetti, 1995; Barchi et al.,
67 1995 and 1998a; Boncio et al., 1998, 2000; Collettini and Barchi, 2002; Brozzetti et al., 2009,
68 Figure 1). In this paper, we report on an AMS study of lower Pleistocene continental clays
69 deposited in the northern sector of the Tiber Basin (High Tiber Valley, Central Apennines), which
70 lies above the ATF, and was formed (and strictly controlled) by the fault activity. Thus, our study
71 provides the first evidence on the magnetic fabric of syn-tectonic sedimentary rocks exposed above
72 a low-angle extensional fault.

73

74 **2. Geologic and tectonic framework of the Altotiberina Fault**

75 During Miocene-Pliocene times an eastward-migrating compressional pulse built up the
76 northern Apennines thrust-and-fold belt, composed by a NE-verging imbricate system (Lavecchia,
77 1988; Ghisetti et al., 1993; Barchi et al., 1998c). During this phase the Tuscan allochthon
78 (Paleogene-Early Miocene pelagites and turbidites) and piggy-back Ligurian Unit (Late Jurassic

79 ophiolites and Cretaceous to Paleogene pelagites and turbidites), overthrust the inner Umbria-
80 Marche Domain (Triassic-Jurassic shelf carbonates and Cretaceous to Miocene pelagites and
81 turbidites).

82 Starting from the Early Pleistocene, extension disrupted the compressional architecture of the
83 axial part of the northern Apennines by NW-SE trending normal faulting, and possibly by minor
84 normal to transtensional features, oriented transversally to the major faults. This last tectonic phase
85 is responsible of the arrangement of most of the Quaternary basins of the region. The most
86 important of these extensional basins in the study area are the High Tiber Valley, to the west, and
87 the intramountain basins of Gubbio and Gualdo Tadino, to the east (Figure 1a).

88 Field and seismic data pointed out the major role played by a regional-scale, low-angle
89 normal fault in the extensional tectonics of the Umbria region: the Altotiberina Fault, one of the
90 best-studied active low-angle normal faults in the world (Figure 1a) (Brozzetti, 1995; Barchi et al.,
91 1995 and 1998a; Boncio et al., 1998 and 2000; Collettini and Barchi, 2002; Brozzetti et al., 2009).
92 The ATF bounds the High Tiber Valley westward and extends for at least 70 km from Sansepolcro
93 to Perugia, with an average NNW–SSE strike and an eastward dip ranging from 20° to 30°. The
94 ATF surface expression, north of Perugia, is composed by a set of normal faults that forms a
95 “domino-like” structure rooted on the east-dipping, low-angle fault plane (Brozzetti, 1995) (Figure
96 1b). Conversely, a high-angle SW-dipping faults array bounds the eastern side of the Quaternary
97 basins, showing a mean NW-SE strike that diverges from the ATF trend. Surface expression of the
98 High Tiber Valley is composed by three en-echelon, NW-SE-elongated sub-basins (Sansepolcro,
99 Umbertide and Ponte Pattoli basins, from NW to SE, see Figure 1a). These basins are separated by
100 morphological thresholds and infilled by a continental depositional sequence that unconformably
101 overlays the Meso-Cenozoic marine sedimentary formations of the northern Apennines (Figure 1a).

102 The analysis of CROP 03 deep seismic profile, as well as of commercial seismic reflection
103 profiles, calibrated using surface geology and borehole data with the aid of geophysical data
104 including gravity, magnetics, heat flow measurements, and tomography, gives a clear picture of the

105 ATF at depth (Boncio et al., 2000; Collettini, 2002; Collettini and Barchi, 2002; Collettini et al.,
106 2000; Pauselli and Federico, 2002; Pauselli et al., 2006). Its geometry has been clearly shown by a
107 well marked reflector that dips toward the east, interrupting the stratigraphic markers down to about
108 13 km (Figure 1c) (Barchi et al., 1995; 1998b), and by the distribution of microseismic activity
109 (Piccinini et al., 2003; Chiaraluce et al., 2007). Seismic reflection profiles show that both synthetic
110 NE- and antithetic SW-dipping normal faults, exposed at the surface, splay out from the ATF,
111 forming an asymmetric graben. A 3D image of the ATF provided by its isobath map (Collettini and
112 Barchi, 2002; Chiaraluce et al., 2007) illustrates a pronounced staircase trajectory and portrays
113 some longitudinal bends, due to attitude variations along its strike.

114 Although most of the fault splays at the surface show displacements on the order of some
115 hundreds of meters, the total displacement on the ATF at depth is about 5 km (Brozzetti et al., 2009;
116 Collettini et al., 2000). The large amount of extension is evidenced from the direct superposition of
117 the Umbria-Marche Miocene turbidites above the Triassic Evaporites, drilled in the Perugia 2 and
118 San Donato wells (Anelli et al., 1994). The geometry of the seismic reflectors of the Quaternary
119 High Tiber Valley bottom suggests a syn-sedimentary tectonics related to the ATF activity that
120 would have produced up to 1200 m-thick sedimentary infill in the Sansepolcro basin (Barchi and
121 Ciaccio, 2009). The oldest exposed sediments indicate an Early Pleistocene onset of extensional
122 activity, though a large part of the syn-tectonic succession is buried and unknown in the central part
123 of the basins. Considering the age of sediments in the basin and the maximum offset of the splay
124 bounding the basin, an average slip rate of 1 mm/a in the past 2 Ma can be estimated (Collettini,
125 2002). Local and regional GPS networks reveal a ~ 3 mm/yr velocity of crustal extension
126 accommodated between the Tyrrhenian and Adriatic coasts. The majority of such extension is
127 concentrated across the High Tiber Valley, with slip rate of 2.4 ± 0.3 mm/yr, and subsidence rate up
128 to 3 mm/yr (Hreinsdóttir and Bennett, 2009).

129 For the Sansepolcro basin, in particular, the seismic data do not show any evidence of
130 compressional structures involving the Quaternary sequence. On the contrary, robust evidence of

131 normal faults propagating through the basin sediments has been recognized: NW–SE-striking
132 mesoscopic normal faults are common within the Early Pleistocene sediments, as well as NE-
133 dipping faults displacing and tilting the Pleistocene sequence (e.g. along the Anghiari Ridge;
134 Cattuto et al., 1995; Delle Donne et al., 2007; ISPRA-CARG Project, Fo. 289). Although sparse,
135 field evidence of normal fault activity has been also detected in the Late Pleistocene–Holocene
136 alluvial terraces (Brozzetti et al., 2009).

137 The geometry and kinematics of these normal faults are consistent with the focal mechanisms
138 of the instrumental earthquakes, indicating a SW–NE active extension, coherent with the regional
139 seismotectonic framework, as defined by both geological and seismological data (e.g. Lavecchia et
140 al., 1994). This suggests that in the study area the extensional tectonics persisted throughout the
141 Quaternary with spatial and temporal continuity, preserving the same regional strain field.

142 The huge amount of geological and geophysical data collected during the last decade (and
143 discussed above) seems to be at odds with the hypothesis that the Tiber basin, as well as other
144 hinterland basins of the central Apennines, is a thrust-top basin (e.g. Boccaletti et al., 1991 and
145 1997; Bonini, 1998). According to these authors, the basins were generated by Pleistocene
146 compressive events, and their bowl-shape is interpreted as a syncline disrupted by Late Pleistocene
147 extensional faulting.

148

149 **3. Sampling and methods**

150 We carried out an extensive AMS study within the three sub-basins composing the High
151 Tiber Valley. Here a complex fluvio-lacustrine Pleistocene sequence, exposed up to a maximum
152 elevation of 350 m above the present valley, shows a progressive incision and disruption, at the
153 hanging-wall of the ATF system (Figure 2). It consists of three depositional cycles, bottom to top:
154 the early Pleistocene Unit, with a prevalent sandy clay sedimentation of marsh to braided river
155 depositional environment; early-middle Pleistocene Unit, with prevalent conglomeratic sediments
156 and some sandy interbodies of fluvial and alluvial depositional environment; the uppermost middle-

157 late Pleistocene Unit, with sparse outcrops of conglomeratic deposits of alluvial fan depositional
158 environment. The lowermost early Pleistocene Unit is unconformably overlain by the early-middle
159 Pleistocene Unit and both are dated by mammal faunas (Ambrosetti et al., 1978, 1987, 1995;
160 Cattuto et al., 1995; Petronio et al. 2002; Argenti, 2004).

161 All sampling sites are from the early Pleistocene Unit and were selected considering the
162 lithology (silty-clayey sediments), the alteration degree (blue-grey coloured sediments indicating a
163 minor weathering), and their relative location, trying to distribute them homogeneously throughout
164 the entire High Tiber Valley. Silty and clayey sediments were sampled at 13 different localities
165 (Figure 2), collecting a total amount of 133 standard cylindrical cores. Eight to thirteen samples,
166 spaced in at least two distinct exposures, were gathered at each site using a petrol-powered portable
167 drill cooled by water. Samples were oriented using a magnetic compass corrected for the local
168 magnetic declination (forecasted at ca. 2° at the time of sampling, Carta Magnetica d'Italia al
169 2005.0).

170 Before the AMS sampling, an extensive 1:10,000-scale geological and geomorphological
171 mapping along the High Tiber Valley was carried out. The field mapping was based on pre-existing
172 geological maps, produced in the framework of previous national (ISPRA-CARG Project, Fo. 288
173 and 289) and/or regional (Regione Umbria) projects, and was aimed at producing an integrated and
174 homogeneous stratigraphic scheme of the continental deposits (< 1.8 Ma in age), that have been
175 characterized also from a sedimentological and structural point of view. The obtained map (Figure
176 1a and Figure 2) was integrated with observations derived from 1:33,000 scale aerial photographs
177 (GAI) and 10 m and 90 m resolution Digital Elevation Models (DEMs).

178 All laboratory analyses were carried out in the paleomagnetic laboratory at the Istituto
179 Nazionale di Geofisica e Vulcanologia (INGV, Rome, Italy). The low-field anisotropy of magnetic
180 susceptibility (AMS) of a specimen per core was measured with a spinner Multi-Function
181 Kappabridge (MFK1-FA, AGICO) using the spinning method. For each sample the measurements
182 allowed to reconstruct the AMS tensor, defined by three eigenvalues (i.e. the maximum,

183 intermediate and minimum susceptibilities) indicated as $k_{\max} \geq k_{\text{int}} \geq k_{\min}$ (or $k_1 \geq k_2 \geq k_3$). The
184 magnetic susceptibility tensor may be represented geometrically by a tri-axial ellipsoid, whose axes
185 are parallel to the eigenvectors of the AMS tensor, that are the maximum, intermediate, and
186 minimum principal susceptibility directions, along which the induced magnetization is strictly
187 parallel to the direction of the applied field. For each specimen, the mean magnetic susceptibility
188 (k_m) is defined as $k_m = (k_1 + k_2 + k_3)/3$.

189 In deformed sediments, the magnetic fabric has proven to serve as a valuable strain proxy when
190 visible strain markers are not recognizable in the field, being the magnetic lineation parallel to the
191 maximum elongation axis (ϵ_1) of the strain ellipsoid (Hrouda and Janak, 1976; Hrouda and Kahan,
192 1991). Previous works carried out on weakly deformed clays from different Italian localities have
193 found that during the incipient stages of deformation the magnetic foliation maintains parallel to the
194 bedding of the strata, whereas the k_{\max} axes tend to cluster parallel to the direction of the fold axes
195 in compressive settings (Sagnotti and Speranza, 1993; Averbuch et al., 1995; Mattei et al., 1997;
196 Sagnotti et al., 1998, Speranza et al., 1999), and perpendicular to the normal faults (i.e. parallel to
197 the stretching direction) in extensional basins (Sagnotti et al., 1994; Mattei et al., 1997, 1999;
198 Cifelli et al., 2004). Consequently, in tilted sequences the magnetic lineation should trend parallel or
199 orthogonal to the local bed strike when forming after compressive or extensional tectonics,
200 respectively. Therefore, the angle between magnetic lineation and local bed dip (or strike) direction
201 is a fundamental parameter that has the potential to discriminate the compressive vs. extensional
202 settings (e.g. Mattei et al., 1997). Furthermore, being the magnetic fabric sensitive to the syn-
203 sedimentary tectonics (e.g., Mattei et al., 1997; Sagnotti et al., 1998), AMS data provide relevant
204 information about the local tectonic regime acting during sedimentation (in our case during the
205 detachment fault formation).

206

207 **4. Results**

208 The AMS ellipsoid and related parameters were evaluated at 12 sites using Jelinek statistics
 209 (Jelinek, 1977, 1978), and results are reported in Table 1 and Figures 2 and 3. The specimen's mean
 210 susceptibility values are quite homogeneous and range from 100 to 266×10^{-6} SI, with a main
 211 clustering around $120\text{-}130 \times 10^{-6}$ SI (Figure 4). Only 3 specimens have a mean magnetic
 212 susceptibility larger than 350×10^{-6} SI (Figure 4), and they all belong to site SANS. The orientation
 213 of the AMS axes for these three specimens is not different from that shown from the other
 214 specimens from the same site.

215 The AMS ellipsoids are well defined at all sites, with eigenvectors well clustered and small
 216 confidence ellipses. The degree of anisotropy and the shape of the AMS ellipsoid were evaluated by
 217 the following parameters (see Jelinek, 1981):

- 218 - Corrected degree of AMS (P') = $\exp\sqrt{\{2[(\eta_1 - \eta)^2 + (\eta_2 - \eta)^2 + (\eta_3 - \eta)^2]\}}$
- 219 - Magnetic lineation (L) = k_1/k_2
- 220 - Magnetic foliation (F) = k_2/k_3
- 221 - Shape parameter (T) = $(2\eta_2 - \eta_1 - \eta_3)/(\eta_1 - \eta_3)$

222 Where, $\eta_1 = \ln k_1$, $\eta_2 = \ln k_2$, $\eta_3 = \ln k_3$, $\eta = (\eta_1 + \eta_2 + \eta_3)/3$.

223 The shape of the AMS ellipsoid is predominantly oblate at our sites ($F > L$ and $T > 0.3$, see
 224 Figure 3a,b, and Table 1). However, three sites (ANS, CAST, GRUC) are characterized by a
 225 moderately oblate AMS ellipsoid ($T \approx 0.2$), one site (RESI) shows a triaxial magnetic fabric ($T \approx 0$),
 226 and one site (MAI) even has a moderately prolate magnetic fabric ($T < 0$), with the magnetic
 227 lineation prevailing over the magnetic foliation (see Table 1). The magnetic foliation was very well
 228 defined, with a tight clustering of k_{\min} axes, at all sites but MAI and GRUC, as discussed below.
 229 The magnetic foliation resulted to be parallel to the bedding plane at sites where the bedding was
 230 clearly recognized in the field. Therefore, we used the magnetic foliation to estimate the bedding
 231 attitude at those sites where it was not clearly measurable in the field.

232 The anisotropy degree (P') is relatively low in our samples, with values always lower than
 233 1.025 (Table 1). Moreover, in our dataset there is no correlation between the anisotropy degree and

234 the mean susceptibility of the individual specimens (Figure 3c). Conversely, the anisotropy degree
235 appears to be correlated to the shape factor (T) for the specimens from site MAI (Figure 5). At sites
236 MAI and GRUC the k_{\max} axes are tightly grouped and define a clear N-S magnetic lineation,
237 whereas the k_{int} and k_{min} axes show a tendency to distribute in a girdle perpendicular to the k_{\max}
238 cluster (Figure 6). Moreover, all the sites (except site SCAS) are characterized by a well-developed
239 magnetic lineation, as documented by limited dispersion of the k_{\max} and k_{int} axes in the magnetic
240 foliation plane (with the semi-angle of the 95% confidence ellipse around the mean k_{\max} axis in the
241 k_{\max} - k_{int} plane (e_{12}) always lower than 30° ; see Table 1). In particular, at nine sites the e_{12} value is
242 even lower than 20° , indicating a very good clustering of k_{\max} axes from the individual specimens.
243 The declinations of the k_{\max} axes from all samples cluster around a mean direction of $N10^\circ$ (Figure
244 3d), though at site level it varies between directions $N303^\circ$ and $N61^\circ$ (Table 1). Moreover,
245 directions of k_{min} axes for all samples indicate that the sampling area is characterized by a general
246 sub-horizontal bedding attitude (Figure 3d), except at sites SCAS and ANS where strata are
247 distinctly tilted (with the azimuth of dip plunging 51° toward the SW and 30° toward the NE,
248 respectively).

249

250 5. Discussion

251 Reliable AMS results have been obtained from the studied area at 12 sites (see Table 1 and
252 Figure 2). The low average value of magnetic susceptibility (162×10^{-6} SI) indicates that the
253 magnetic susceptibility mainly reflects the contribution of the paramagnetic matrix and that the
254 AMS fabric is mostly determined by the preferred orientation of the clay minerals (Rochette, 1987;
255 Averbuch et al., 1995; Sagnotti et al., 1998; Speranza et al., 1999; Maffione et al., 2010). Moreover,
256 since the AMS anisotropy degree of a rock can also be a function of the intrinsic susceptibility of
257 the composing minerals (e.g., Rochette et al, 1992; Borradaile and Jackson, 2004), the lack of
258 correlation between P' and the k_m observed in our dataset (Figure 3c) indicates that the degree of
259 magnetic anisotropy is not controlled by variations in the magnetic mineralogy.

260 It is well known that the AMS anisotropy degree (P') in deformed sediments may be related to the
261 strain degree of a rock during progressive deformation and metamorphism (e.g., Hrouda and Janak,
262 1976; Hrouda and Kahan, 1991). The P' values observed in our samples are within the typical range
263 of variability for completely undeformed sediments or for sediments at the very early stages of
264 deformation (e.g., Hrouda, 1982; Pares, 2004). These values are generally lower than those
265 measured for other weakly deformed clays in the Italian peninsula (Sagnotti and Speranza, 1993;
266 Sagnotti et al., 1994, 1998; Mattei et al., 1999; Maffione et al., 2008).

267 A prevalent oblate shape of AMS ellipsoids, with k_{\min} axes clustered perpendicular to the
268 bedding plane indicates that the sampled sediments mostly preserve a predominant sedimentary-
269 compactional AMS fabric (e.g., Tarling and Hrouda, 1993). Actually, in low-energy environments
270 such as the marshes where the studied clayey sediments were deposited, gravity-driven
271 sedimentation brings platy grains to lay with their longer dimensions statistically parallel to the
272 bedding-compaction plane. Then, with further sediment burial, the effect of diagenetic compaction
273 on platy minerals by pressure and water expulsion reinforces the parallelism between the magnetic
274 foliation and the bedding plane. The inference of a prevalent depositional-compactional AMS fabric
275 is in agreement with field observations, given that no clear macroscopic pervasive deformation
276 related to tectonics was noticed at the sampling sites.

277 The clustering of the k_{\max} axes observed at all sites also defines a distinct magnetic lineation
278 which, in absence of water currents, can not be related to sedimentary processes. Analogously to
279 other weakly deformed mudstones in various compressional and extensional settings, this magnetic
280 lineation may rather be interpreted as the first effect of a superimposed strain field. In particular, the
281 AMS fabric of sites MAI and GRUC, with a tendency toward prolate AMS ellipsoids and a
282 scattering of k_{int} and k_{\min} axes in a girdle perpendicular to the cluster of k_{\max} axes (Figure 6) clearly
283 indicates that at those sites the original sedimentary-compactional fabric was largely overprinted by
284 a pervasive tectonic deformation that affected the preferred orientation distribution of the clay
285 matrix. This is a clear tectonic effect that occurs when mineral rotations are developed enough to

286 bring clay flakes to a high angle to the shortening direction and to impart a magnetic fabric typical
287 of the “pencil structure” stage (e.g., Graham, 1966; Pares, 2004). At these two sites the k_{\min} axes
288 can not be used to estimate the bedding attitude.

289 Our results are the first AMS data gathered from a basin formed due to activity of a low-angle
290 normal fault (i.e., the ATF) and represent a valuable tool for the characterization of the tectonic
291 stress acting on the shallow hanging-wall of such detachment fault. A clear magnetic foliation sub-
292 parallel to the bedding planes is observed at all sampled sites. Five out of twelve sites have a sub-
293 horizontal bedding attitude (dip $\leq 5^\circ$) (see Figure 2, and Table 1). However, the relationship between
294 the orientation of the magnetic lineation and the bedding attitude (which may discriminate the
295 compressive vs. extensional origin of the magnetic lineation) can be evaluated for the six sites
296 characterized by a clear bed dip ($>5^\circ$, Table 1 and Figure 6). In such six sites the magnetic lineation,
297 trending NE to NNW (\sim N-S on average), is sub-parallel to local bed strike direction, as always
298 observed in folds of compressive tectonic settings. This has three important implications: 1) the
299 sediments of the High Tiber Valley deposited above the ATF are arranged in incipient, local folds
300 that are hardly visible in the field; 2) fold axes are predominantly sub-parallel to the trend of the
301 ATF (except at sites SANS, SCAS, TER and RESI); 3) folds are routinely considered as proofs for
302 shortening and associated to thrust-sheet emplacement, while here they developed in the purely
303 extensional regime of the ATF.

304 Magnetic lineations of the remaining five sub-horizontal sites trend both NW to NNW (sites
305 CAST, CAV, and MON, Figure 2), and NE (sites SANS and TER; Table 1 and Figure 2). Being the
306 angle between the magnetic lineation and the bedding strike not inferred at these sites, the origin of
307 the magnetic lineation was interpreted on the basis of their relative direction with respect to the
308 regional stress field active during the fault activity. Accordingly, a compressional magnetic
309 lineation characterizes sites CAST, CAV, and MON, while an extensional magnetic lineation is
310 observed at sites SANS and TER. In particular, sites SANS and TER occur on the western side and
311 in the axial parts of the two en-echelon Sansepolcro and Umbertide basins, respectively, and the

312 inferred stretching direction (i.e. NE-SW) is compatible with the regional extensional strain induced
313 by the ATF system.

314 In general, our data show a coexistence of both compressional and extensional strain field that
315 affected the coeval, early Pleistocene deposits lying over the shallow hanging-wall of the ATF. The
316 existence of compressive structures in extensional settings characterized by low-angle extensional
317 faults has been already documented elsewhere, and studied in detail at the Basin and Range
318 province (Schlische, 1995; Janecke et al., 1998). These authors suggested the possibility to have
319 folds in extensional regime through eight different mechanisms. These mechanisms are grouped by
320 the geometry of the resulting fold, which can be characterized by axis parallel (“longitudinal”),
321 orthogonal (“transverse”), or “oblique” to the associated normal fault. Models concerning the
322 formation of oblique folds (Janecke et al., 1998) consider (i) the local effects related to a non planar
323 fault surface, (ii) the transtensional strain, or (iii) a simultaneous effect of the longitudinal and
324 transverse mechanisms, as possible driving mechanism. Furthermore, recent numerical modelling
325 on extensional faults (e.g. Bott, 2009) have demonstrated that the uppermost part (~4 km) of the
326 hanging-wall block is dominated by a widespread, horizontal compressive stress.

327 In the past, two incompatible views of the Plio-Pleistocene tectonics of the Tiber basin were put
328 forward: the first interpreted the Plio-Pleistocene sediments as deposited in purely extensional post-
329 collisional syn-rift basins (Barchi et al., 1999, 2009; Collettini et al., 2000), while the second argued
330 for compressive pulses punctuating the extensional tectonics (Bernini et al., 1990; Boccaletti et al.,
331 1992, 1994 and 1997; Bonini, 1998; Bonini and Tanini, 2009). Our data suggest the presence on the
332 shallow hanging-wall of the ATF of synchronous, local extensional and compressional strain acting
333 during the early Pleistocene and compatible with the regional extensional tectonics. This local strain
334 is probably induced by the presence of ATF plane irregularities (longitudinal bends and staircase
335 trajectory at depth), as clearly portrayed by seismic reflections profiles (Collettini and Barchi, 2002;
336 Chiaraluce et al., 2007; Barchi et al., 2009), and should not be interpreted as the result of late
337 Miocene-Quaternary compressive events (as proposed in the past). The same interpretation could be

338 applied to similar compressive structures observed in other sedimentary basins of Tuscany lying on
339 top of low-angle extensional faults (Ambrosetti et al., 1978; Bernini et al., 1990; Boccaletti et al.,
340 1992, 1994; Collettini et al., 2006). Further AMS studies of the Plio-Quaternary sediments from the
341 High Tiber Valley and similar basins of the central Apennines would be needed to unravel the
342 regional vs. local origin of such compressive structures, and possibly reconstruct the regional stress
343 field acting in areas where low-angle detachment faults occur.

344

345 **6. Conclusion**

346 The Pleistocene continental clayey sediments sampled in the High Tiber Valley are
347 characterized by a well-developed magnetic fabric. The AMS data collected in our study indicate
348 that the original sedimentary-compactional fabric of these sediments has been partly overprinted by
349 strain effects linked to the activity of the Altotiberina low-angle normal fault. As concluding
350 remarks of our study, we stress that:

- 351 • AMS data from lower Pleistocene clays of the High Tiber basin are consistent with both
352 structural evidence gathered in the past from the Basin and Range detachment fault
353 system and numerical modelling, and clearly document that the hanging-wall of a low-
354 angle extensional fault can be characterized by incipient folds, developed in function of
355 the non-planarity of the detachment fault at depth.
- 356 • The exposure conditions of the clayey sediments of the High Tiber Valley (vegetated or
357 yielding Bad Lands) are unsuitable to clearly detect these compressive structures in the
358 field. Thus, our results confirm the potentiality of AMS to reveal hidden tectonic
359 features characterizing mildly deformed sediments which appear undeformed at the
360 outcrop scale.
- 361 • According to our interpretation, the long-standing opposite views on the late Miocene-
362 Pleistocene tectonics of the internal northern Apennines (extensional vs. compressive)
363 can now be reconciled by considering the occurrence of compressive features as local

364 effects linked to the activity of low-angle normal faults dipping toward the NE beneath
 365 the chain.

366

367 **7. Acknowledgements**

368 It is a pleasure and an honour for us to contribute to the volume celebrating the scientific career of
 369 Prof. František Hrouda, in recognition of his fundamental contribution to the research on the
 370 magnetic anisotropy of rocks and its application in geophysics. This work has been carried out in
 371 the framework of the *INGV-DPC 2007-2009 Seismological Projects*, S5 “Test-sites:Altotiberina
 372 normal fault” WP 1.5, and INGV funds.

373

374

375 **References**

376

- 377 Ambrosetti, P., M.G., Carboni, M.A., Conti, A., Costantini, D., Esu, A., Gadin, O., Girotti, A., Lazzarotti, R., Mazzanti,
 378 U., Nicosia, G., Parisi, F., Sandrelli, 1978. Evoluzione paleogeografica e tettonica dei bacini tosco-umbro-laziali
 379 nel Pliocene e nel Pleistocene inferiore. *Mem. Soc. Geol. Ital.* 19, 573–580.
- 380 Anelli, L., Gorza, M., Pieri, M., Riva, M., 1994. Subsurface well data in the northern Apennines (Italy). *Mem. Soc.*
 381 *Geol. Ital.* 48, 461–471.
- 382 Argenti, P. (2004). Plio-quaternary mammal fossiliferous sites of Umbria (Central Italy). *Geologica Romana*(2003-
 383 2004) 37, 67-78.
- 384 Averbuch, O., Mattei, M., Kissel, C., Frizon de Lamotte, D., Speranza, F., 1995. Cinématique des déformations au sein
 385 d’un système chevauchant aveugle: l’exemple de la “Montagna dei Fiori” (front des Apennins centraux, Italie),
 386 *Bull. Soc. Géol. France*, 5, 451–461.
- 387 Barchi, M.R., M.G. Ciaccio, 2009. Seismic images of an extensional basin, generated at the hanging-wall of a low-
 388 angle normal fault: The case of the Sansepolcro basin (Central Italy). *Tectonophysics*, 479, 285-293.
- 389 Barchi, M.R., Magnani, M.B., Minelli, G., Piali, G., Ponziani, F., Sotera, B.M., 1995. Osservazioni geofisiche sul
 390 basamento della regione umbro-marchigiana. *Atti del 12° Convegno del Gruppo Nazionale di Geofisica della*
 391 *Terra Solida*, pp. 709–720.
- 392 Barchi, M.R., Minelli, G., and Piali, G., 1998a, The CROP 03 profile: A synthesis of results on deep structures of the
 393 Northern Apennines: *Memorie della Società Geologica Italiana*, v. 52, p. 383–400.
- 394 Barchi, M.R., De Feyter, A., Magnani, M.B., Minelli, G., Piali, G., Sotera, B.M., 1998b. Extensional tectonics in the
 395 Northern Apennines (Italy): Evidence from the CROP03 deep seismic reflection line. *Mem. Soc. Geol. It.* 52,
 396 527–538.
- 397 Barchi M., De Feyter A., Magnani M.B., Minelli G., Piali G. & Sotera B.M., 1998c. The structural style of the Umbria-
 398 Marche fold and thrust belt. *Mem.Soc.Geol.It.* 52, 557-578.

- 399 Barchi, M.R., S., Paolacci, C., Pauselli, G., Piali, S., Merlini, 1999. Geometria delle deformazioni estensionali recenti
400 del bacino dell'Alta Val Tiberina fra S. Giustino Umbro e Perugia: evidenze geofisiche e considerazioni
401 geologiche. *Boll. Soc. Geol. Ital.* 118, 617– 625.
- 402 Bernini, M., Boccaletti, M., Moratti, G., Papani, G., Sani, F., Torelli, L., 1990. Episodi compressivi neogenico-
403 quaternari nell'area estensionale tirrenica nord-orientale. *Dati in mare e a terra. Mere. Soc. Geol. Ital.* 45, 577-
404 589.
- 405 Boccaletti, M., A., Cenina-Feroni, P., Martinelli, G., Moratti, G., Plesi, F. and Sani, 1992. Late Miocene-Quaternary
406 compressive events in the Tyrrhenian side of the Northern Apennines. *Ann. Tectonicae*, 4, 214-230.
- 407 Boccaletti, M., A., Cerrina Feroni, P., Martinelli, G., Moratti, G., Plesi, and F. Sani, F., 1994. L'area tosco-laziale come
408 dominio di transizione tra il bacino tirrenico e i thrusts esterni: rassegna di dati mesostrutturali e possibili
409 relazioni con le discontinuità del "Ciclo Neoautoctono". *Mem. Descr. Carta Geol. Ital.*, 49, 9-22.
- 410 Boccaletti, M., G. Gianelli, F. Sani, 1997. Tectonic regime, granite emplacement and crustal structure in the inner zone
411 of the northern Apennines (Tuscany, Italy): a new hypothesis. *Tectonophysics*, 270, 127-143.
- 412 Boncio, P., Brozzetti, F., Ponziani, F., Barchi, M., Lavecchia, G., Piali, G., 1998. Seismicity and extensional tectonics in
413 the northern Umbria-Marche Apennines. *Mem. Soc. Geol. It* 52, 539±555.
- 414 Boncio, P., Brozzetti, F., Lavecchia, G., 2000. Architecture and seismotectonics of a regional low-angle normal fault
415 zone in central Italy. *Tectonics* 19, 1038–1055.
- 416 Bonini, M., 1998. Chronology of deformation and analogue modelling of the Plio-Pleistocene "Tiber Basin":
417 implications for the evolution of the Northern Apennines (Italy). *Tectonophysics*, 285, 147-165.
- 418 Bonini, M. and C. Tanini, 2009. Tectonics and Quaternary evolution of the Northern Apennines watershed area (upper
419 course of Arno and Tiber rivers, Italy). *Geological Journal*, 44, 2–29, DOI: 10.1002/gj.1122
- 420 Borradaile, G.J., 1988, Magnetic susceptibility, petrofabrics and strain, *Tectonophysics*, 156 (1-2), 1-20, DOI:
421 10.1016/0040-1951.
- 422 Borradaile, G.J., and M. Jackson, 2004. Anisotropy of magnetic susceptibility (AMS): magnetic petrofabrics of
423 deformed rocks. In Martín-Hernández, F., Lüneburg, C., Aubourg, C., and Jackson, M., (eds.), *Magnetic Fabric
424 Methods and Applications*. Geological Society, London, Special Publications 2004; v. 238, pp. 299–360.
- 425 Borradaile, G.J., B. Henry, 1997, Tectonic applications of magnetic susceptibility and its anisotropy, *Earth Science
426 Reviews*, 42 (1-2), 49-93, DOI: 10.1016/S0012-8252.
- 427 Bott, M.H.P., 2009. Stresses in planar normal faulting: shallow compression caused by fault-plane mismatch. *J. Stru.
428 Geol.*, 31, 354–365.
- 429 Brozzetti, F., 1995. Stile deformativo della tettonica distensiva nell'Umbria Occidentale: l'esempio dei Massicci
430 Mesozoici Perugini. *Studi Geologici Camerti*, Vol. Spec 1995/1, 105±119.
- 431 Brozzetti, F., P. Boncio, G. Lavecchia, B. Pace, 2009. Present activity and seismogenic potential of a low-angle normal
432 fault system (Città di Castello, Italy): Constraints from surface geology, seismic reflection data and seismicity,
433 *Tectonophysics* 463, 31–46.
- 434 Carta Magnetica d'Italia al 2005.0, CD-ROM, Istituto Nazionale di Geofisica e Vulcanologia (INGV), Rome, Italy.
- 435 Cattuto, C., Cencetti, C., Fisauli, M., Gregori, L., 1995. I bacini pleistocenici di Anghiari e Sansepolcro nell'alta valle
436 del Tevere. *Il Quaternario* 8, 119±128.
- 437 Chiaraluce, L., Charabba, C., Collettini, C., and Cocco, M., 2007, Architecture and mechanics of an active low-angle
438 normal fault: Alto Tiberina Fault, northern Apennines, Italy: *Journal of Geophysical Research*, v. 112, B10310,
439 doi: 10.1029/2007JB005015.

- 440 Cifelli F., M. Mattei, A.M. Hirt, A. Günther (2004), The origin of tectonic fabrics in “undeformed” clays: The early
 441 stages of deformation in extensional sedimentary basins, *Geophys. Res. Lett.*, 31(9), doi:
 442 10.1029/2004GL019609.
- 443 Collettini C., N., De Paola R.E., Holdsworth M.R., Barchi, 2006. The development and behaviour of low-angle normal
 444 faults during Cenozoic asymmetric extension in the Northern Apennines, Italy. *J. Struct. Geol.*, 28, 333-352.
- 445 Collettini, C., 2002, Hypothesis for the mechanics and seismic behaviour of low-angle normal faults: The example of
 446 the Altotiberina fault Northern Apennines: *Annals of Geophysics*, v. 45, p. 683–697.
- 447 Collettini, C., M.R., Barchi, 2002. A low-angle normal fault in the Umbria region (Central Italy): A mechanical model
 448 for the related microseismicity. *Tectonophysics*, 359, 97–115, doi: 10.1016/S0040-1951(02)00441-9.
- 449 Collettini, C., M.R., Barchi, C., Pauselli, C., Federico, G., Pialli, 2000. Seismic expression of active extensional faults
 450 in northern Umbria (central Italy). In: Cello, G., Tondi, E. (Eds.), *The Resolution of Geological Analysis and*
 451 *Models for Earthquake Faulting Studies. Journal of Geodynamics*, 29, 309– 321.
- 452 Delle Donne, D., Piccardi, L., Odum, J.K., Stephenson, W.J., Williams, R.A., 2007. Highresolution shallow reflection
 453 seismic image and surface evidence of the Upper Tiber Basin active faults (Northern Apennines, Italy). *Boll.*
 454 *Soc. Geol. Ital. (Ital.J. Geosci)* 126 (2), 323–331.
- 455 Faccenna, C., Speranza, F., D’Ajello Caracciolo, F., Mattei, M., Oggiano, G. (2002). Extensional tectonics on Sardinia
 456 (Italy): insights into the arc-back-arc transitional regime. *Tectonophysics*, 356, 213-232.
- 457 Ghisetti F., Barchi M., Bally A.W., Moretti I. & Vezzani L.(1993) - Conflicting balanced structural sections across the
 458 central Apennines (Italy): problems and implications. In: A. M. Spencer (Editor): "Generation, Accumulation and
 459 Production of Europe's Hydrocarbons III". *European Assoc. Petrol. Geol., Special Publication*, 3, 219-231,
 460 Springer-Verlag, Berlin, Heidelberg.
- 461 Gradstein, F.M., J.G. Ogg, and A.G. Smith, 2004. *A Geologic Time Scale 2004*, Cambridge University Press, pp. 589.
- 462 Graham, J.W., 1966. Significance of magnetic anisotropy in Appalachian sedimentary rocks. In: Steinhart, J.S., and
 463 Smith, T.J. (eds.), *The Earth Beneath the Continents. Geophysical Monograph Series 10*. Washington, DC:
 464 American Geophysical Union, pp. 627–648.
- 465 Hreinsdóttir, S., and Bennett, R.A., 2009. Active aseismic creep on the Alto Tiberina low-angle normal fault, Italy.
 466 *Geology* 37; 683-686, doi: 10.1130/G30194A.1
- 467 Hrouda, F. and F. Janák, 1976. The changes in shape of the magnetic susceptibility ellipsoid during progressive
 468 metamorphism and deformation. *Tectonophysics*, 34, 135-148.
- 469 Hrouda, F., 1982. Magnetic anisotropy of rocks and its application in geology and geophysics. *Surveys in geophysics*, 5
 470 (1), 37-82, DOI: 10.1007/BF01450244.
- 471 Hrouda, F., S. Kahan, 1991. The magnetic fabric relationship between sedimentary and basement nappes in the High
 472 Tatra Mts. (N Slovakia). *J. Struct. Geol.*, 13, 431-442.
- 473 ISPRA-Carg Project - Sheet 289 “Città di Castello” of the Carta Geologica d'Italia, in press by APAT; pre print at
 474 <http://www.apat.gov.it/Media/carg/index.html>.
- 475 Janecke, S., C.J. Vandenburg, J.J. Blankenau, 1998. Geometry, mechanisms and significance of extensional folds from
 476 examples in the Rocky Mountain Basin and Range province, USA. *Journal of Structural Geology*, 20 (7), 841-
 477 856.
- 478 Jelinek, V. (1977), *The statistical theory of measuring anistropy of magnetic susceptibility of rocks and its application*,
 479 *Geofyzika*, Brno, pp. 88.

- 480 Jelinek, V. (1978), Statistical processing of magnetic susceptibility on groups of specimens, *Stud. Geophys. Geod.* 22,
481 50–62.
- 482 Jelinek, V. (1981), Characterization of the magnetic fabric of rocks. *Tectonophysics*, 79, 63-67.
- 483 Lavecchia, G., 1988. The Tyrrhenian-Apennines system: structural setting and seismotectogenesis. *Tectonophysics*,
484 147,263-296.
- 485 Lavecchia, G., Brozzetti, F., Barchi, M.R., Keller, J.V.A., Menichetti, M., 1994. Seismotectonic zoning in east-central
486 Italy deduced from the analysis of the Neogene to present deformations and related stress fields. *Geol. Soc.*
487 *Amer. Bull.* 106, 1107–1120.
- 488 Maffione, M., F. Speranza, C. Faccenna, A. Cascella, G. Vignaroli, and L. Sagnotti (2008), A synchronous Alpine and
489 Corsica-Sardinia rotation, *J. Geophys. Res.*, 113, B03104, doi:10.1029/2007JB005214.
- 490 Maffione, M., F. Speranza, C. Faccenna, E. Rossello, 2010. Paleomagnetic evidence for a pre-early Eocene (~50 Ma)
491 bending of the Patagonian orocline (Tierra del Fuego, Argentina): Paleogeographic and tectonic implications.
492 *Earth and Planetary Science Letters*, 289, 273–286.
- 493 Mattei, M., F. Speranza, A. Argentieri, F. Rossetti, L., Sagnotti, and R. Funicello, (1999), Extensional tectonics in the
494 Amantea basin (Calabria, Italy): A comparison between structural and magnetic anisotropy data. *Tectonophysics*,
495 307, 33-49.
- 496 Mattei, M., L. Sagnotti, C. Faccenna, R. Funicello, (1997), Magnetic fabric of weakly deformed clay-rich sediments in
497 the Italian peninsula: Relationship with compressional and extensional tectonics. *Tectonophysics*, 271, 107-122.
- 498 Pares, J. (2004), How deformed are weakly deformed mudrocks? Insights from magnetic anisotropy, *Geological*
499 *Society, London, Special Publications*, Vol. 238, 191-203, doi:10.1144/GSL.SP.2004.238.01.13
- 500 Pares, J.M., Van der Pluijm, B.A., Dinares-Turell, J., (1999), Evolution of magnetic fabrics during incipient
501 deformation of mudrocks (Pyrenees, northern Spain). *Tectonophysics*, 307, 1-14.
- 502 Pauselli, C., and Federico, C., 2002, The brittle/ductile transition along the CROP03 seismic profile: Relationship with
503 the geological features: *Bollettino della Società Geologica Italiana*, v. 1, p. 25–35.
- 504 Pauselli, C., Barchi, M.R., Federico, C., Magnani, M.B., and Minelli, G., 2006, The crustal structure of the Northern
505 Apennines (Central Italy): An insight by the CROP03 seismic line: *American Journal of Science*, v. 306, p. 428–
506 450.
- 507 Petronio, C., P. Argenti, L. Caloi, D. Esu, O. Girotti, R. Sardella (2002). Updating Villafranchian mollusc and mammal
508 faunas of Umbria and Latium (Central Italy) *Geologica Romana* (2000-2002) 36, 369-387.
- 509 Piccinini, D., Cattaneo, M., Chiarabba, C., Chiaraluca, L., De Martin, M., Di Bona, M., Moretti, M., Selvaggi, G.,
510 Augliera, P., Spallarossa, D., Ferretti, G., Michelini, A., Govoni, A., Di Bartolomeo, P., Romanelli, M., Fabbri,
511 J., 2003. A microseismic study in a low seismicity area of Italy: the Città di Castello 2000–2001 experiment.
512 *Ann. Geophys.* 46 (6), 1315–1324.
- 513 Rochette, P., 1987. Magnetic susceptibility of the rock matrix related to magnetic fabric studies. *J. Struct. Geol.*, 9,
514 1015-1020.
- 515 Rochette, P., M.J. Jackson, C. Aubourg, 1992. Rock magnetism and the interpretation of anisotropy of magnetic
516 susceptibility, *Rev. Geophys.*, 30(3), 209-226.
- 517 Sagnotti, L., C. Faccenna, R. Funicello, and M. Mattei (1994), Magnetic fabric and structural setting of Plio-
518 Pleistocene clayey units in an extensional regime: the Tyrrhenian margin of Central Italy, *J. Structural Geology*,
519 16, 1243-1257.

- 520 Sagnotti, L., Speranza, F., (1993), Magnetic fabric analysis of the Plio-Pleistocene clayey units of the Sant'Arcangelo
521 basin, southern Italy. *Physics of the Earth and Planetary Interiors*, 77, 165-176.
- 522 Sagnotti, L., Speranza, F., Winkler, A., Mattei, M., Funicello, R., 1998. Magnetic fabric of clay sediments from the
523 external northern Apennines (Italy). *Phys. Earth Planet. Inter.* 105, 73-93.
- 524 Schlische, R.W., 1995. Geometry and origin of fault-related folds in extensional settings. *American Association of*
525 *Petroleum Geologists Bulletin*, 79, 1661-1678.
- 526 Speranza, F., Maniscalco, R., Mattei, M., Di Stefano, A., Butler, R.W.H., Funicello, R., 1999. Timing and magnitude
527 of rotations in the frontal thrust systems of southwestern Sicily. *Tectonics* 18(6), 1178-1197.
- 528 Tarling, D.H., F Hrouda, 1993, *The magnetic anisotropy of rocks*, Chapman and Hall, London, 217 pp.
- 529
- 530
- 531

532 **Figure captions**

533

534 **Figure 1.** a) Simplified geological map of the study area; b) Geological cross-section through the
535 High Tiber Valley from surface and subsurface data (see location in Fig. 1,c) (from Collettini and
536 Barchi, 2002); c) The Altotiberina Fault imaged by a seismic reflection profile (from Boncio et al.,
537 2000).

538

539 **Figure 2.** Geological e structural map of the High Tiber Valley showing stereoplots of AMS (in situ
540 coordinates) for all sampled sites. Larger symbols and ellipses in stereoplots are the mean values
541 and the confidence ellipses for the k_{\min} , k_{int} , and k_{\max} axes, respectively.

542

543 **Figure 3.** AMS results from the 115 studied specimens. (a) Lineation (L) vs. foliation (F) plot. (b)
544 Shape factor (T) vs. anisotropy degree (P'). (c) Anisotropy degree (P') vs. bulk susceptibility (K_m).
545 (d) Lower hemisphere equal-area projection of the k_{\max} and k_{\min} axes of the AMS ellipsoid (in-situ
546 coordinates) and their mean values (larger symbols).

547

548 **Figure 4.** Frequency distribution of the mean susceptibility (k_m) values for all the measured
549 specimens.

550

551 **Figure 5.** Anisotropy degree (P') versus shape factor (T) diagrams of site MAI showing a possible
552 tectonics-related correlation.

553

554 **Figure 6.** Stereoplots of the AMS for the sites showing features of sediments weakly deformed
555 under a compressional strain, that is a magnetic lineation trending parallel to the local strike of the
556 bedding or a “pencil fabric” with k_2 and k_3 axes scattered in the plane normal to the direction

557 defined by the clustering of the k_1 axes. Mean values (larger symbol) and confidence ellipses are
558 also shown for each stereoplot.

Table 1. Anisotropy of magnetic susceptibility results from the High Tiber Valley.

Site	Coordinates		Bedding Az Dip / Dip	n/N	K _m (10 ⁻⁶ SI)	L	F	P'	T	D(°)	I(°)	e ₁₂ (°)
	Latitude N	Longitude E										
SANS	4823174	265743	298/2	10/11	266	1.004	1.015	1.019	0.608	241.2	1.2	14.5
SCAS	4814054	275775	121/51	12/12	111	1.001	1.016	1.020	0.862	207.7	4.4	50.5
CAST	4812770	278793	178/1	9/10	114	1.008	1.011	1.021	0.221	179.4	0.8	4.3
CAV	4812032	278395	259/4	10/11	127	1.004	1.018	1.024	0.563	346.9	0.2	14.5
GRUC	4810111	279378	-	11/11	157	1.004	1.006	1.010	0.231	173.5	1.6	12.7
MAI	4809428	279019	065/15 (*)	10/10	179	1.004	1.003	1.008	-0.158	355.0	4.7	27.0
TER	4804301	279519	058/5	10/13	209	1.004	1.016	1.021	0.646	39.5	5.0	7.5
MON	4805788	282856	192/3	7/8	101	1.001	1.009	1.011	0.732	123.1	1.3	27.8
ANS	4803116	282165	069/30	9/11	230	1.005	1.006	1.010	0.109	354.0	8.1	13.5
UMB	4799694	286417	266/12	10/11	149	1.001	1.003	1.004	0.655	346.7	2.1	17.1
PIE	4793247	289282	079/10	7/11	120	1.006	1.012	1.018	0.350	161.8	1.2	5.4
RESI	4786379	291594	279/17	10/10	172	1.010	1.011	1.021	0.073	188.5	2.7	9.5

Geographic coordinates are in WGS84 datum (UTM projection, zone 33N). Formation age is referred to the Geologic Time Scale from Gradstein et al. (2004). n/N, number of samples giving reliable results/number of studied samples at a site. Bedding attitude is inferred from the site mean direction of K_{\min} axes. K_m , L and F, are mean magnetic susceptibility, magnetic lineation and foliation values, respectively. P' and T are the corrected anisotropy degree and shape factor, respectively, according to Jelinek (1981). D and I are the in situ site mean declination and inclination, respectively, of the maximum susceptibility axis (k_{\max}). e_{12} is the semi-angle of the 95% confidence ellipse around the mean K_{\max} axis in the K_{\max} - K_{\min} plane.

(*) Bedding attitude at this site has been measured in the field.

Figure 1

[Click here to download Figure: figure 1_geology_LD.eps](#)

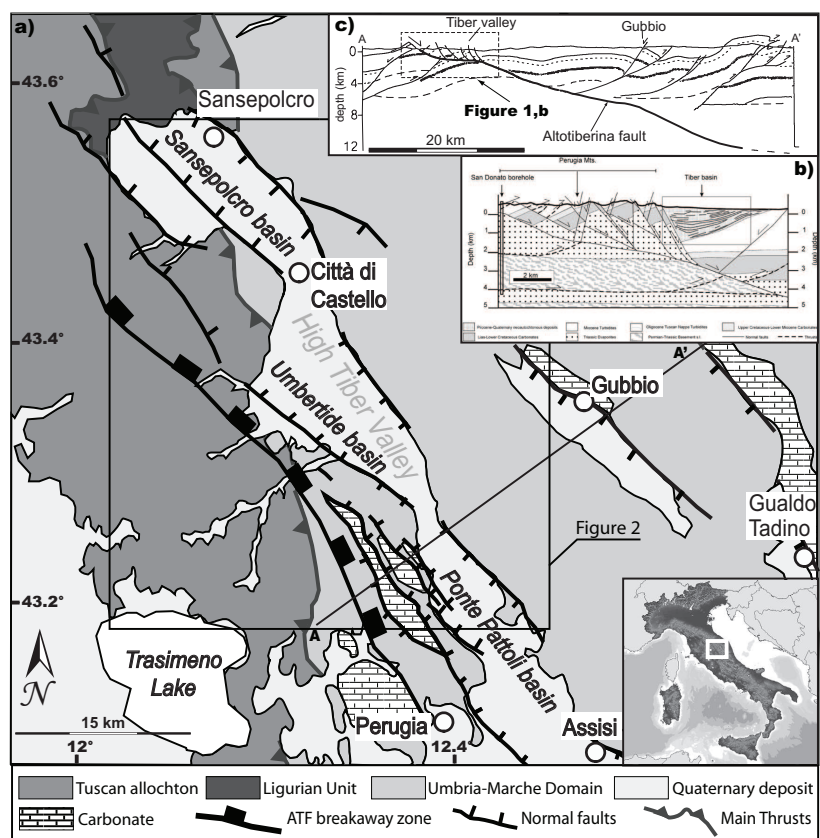


Figure 2
[Click here to download Figure: Figure 2_PlotMap_marco.eps](#)

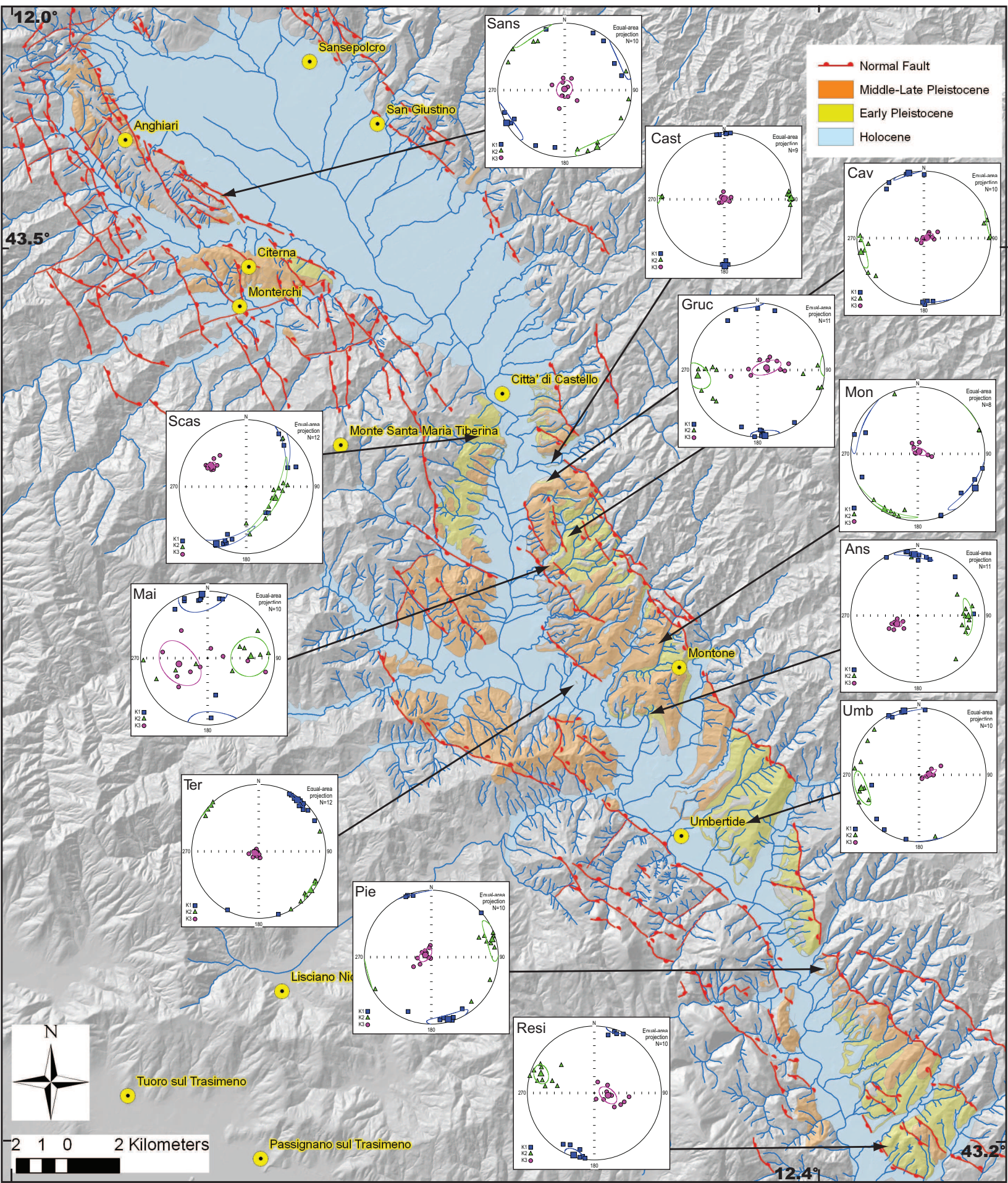


Figure 3
[Click here to download Figure: Figure 3_AMS results.eps](#)

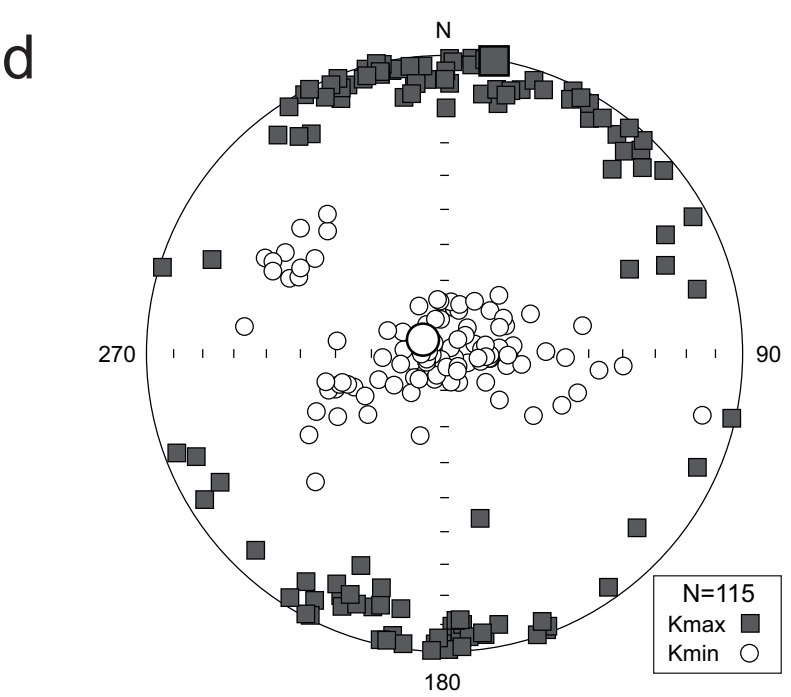
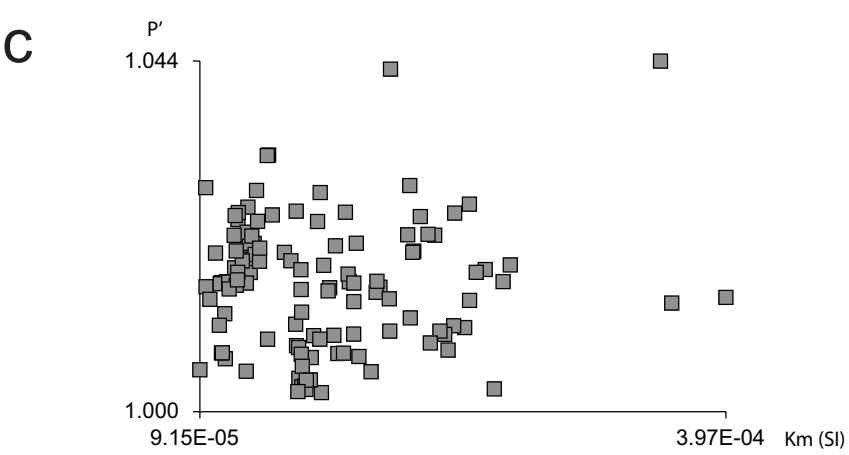
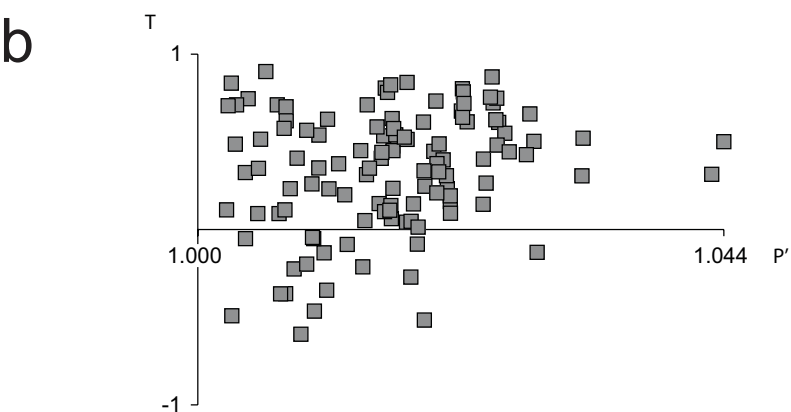
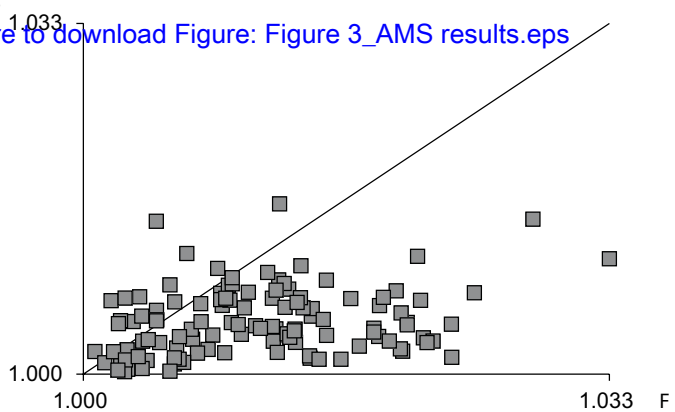


Figure 4
[Click here to download Figure: Figure 4_freq_distr.eps](#)

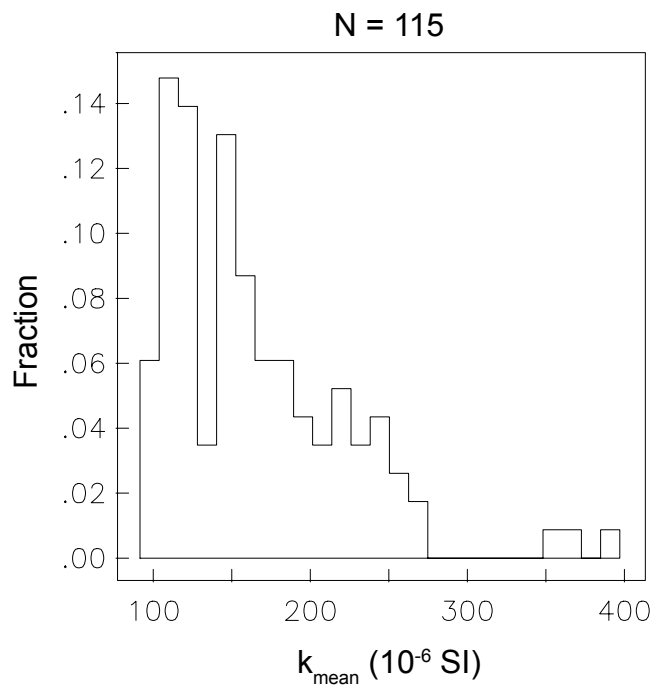


Figure 5

[Click here to download Figure: Figure 5_TvsP.eps](#)

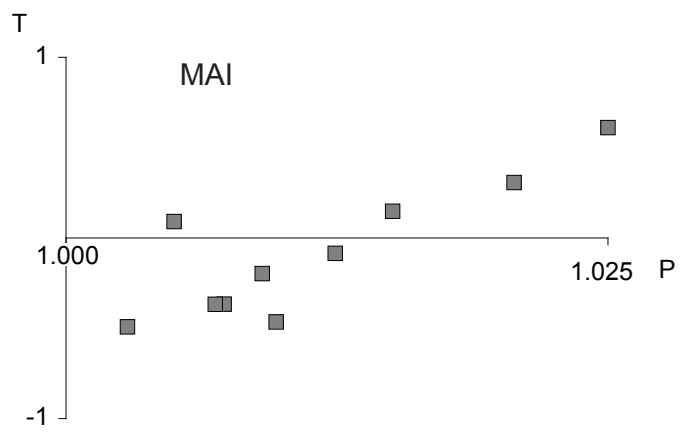


Figure 6
[Click here to download Figure: Figure 6_Plot_specific.eps](#)

